



LAWRENCE  
LIVERMORE  
NATIONAL  
LABORATORY

# Neutron induced inelastic cross sections of $^{150}\text{Sm}$ for $E_n = 1$ to 35 MeV

D. Dashdorj, G. E. Mitchell, T. Kawano, J. A. Becker, U. Agvaanluvsan, M. B. Chadwick, J. R. Cooper, M. Devlin, N. Fotiades, P. E. Garrett, R. O. Nelson, C. Y. Wu, W. Younes

August 18, 2006

19-th Intl. Conference on the Application of Accelerators in  
Research and Industry  
Forth Worth, TX, United States  
August 20, 2006 through August 25, 2006

## **Disclaimer**

---

This document was prepared as an account of work sponsored by an agency of the United States Government. Neither the United States Government nor the University of California nor any of their employees, makes any warranty, express or implied, or assumes any legal liability or responsibility for the accuracy, completeness, or usefulness of any information, apparatus, product, or process disclosed, or represents that its use would not infringe privately owned rights. Reference herein to any specific commercial product, process, or service by trade name, trademark, manufacturer, or otherwise, does not necessarily constitute or imply its endorsement, recommendation, or favoring by the United States Government or the University of California. The views and opinions of authors expressed herein do not necessarily state or reflect those of the United States Government or the University of California, and shall not be used for advertising or product endorsement purposes.

# Neutron induced inelastic cross sections of $^{150}\text{Sm}$ for $E_n = 1$ to 35 MeV

D. Dashdorj<sup>1,2,\*</sup>, G.E. Mitchell<sup>1,3</sup>, T. Kawano<sup>4</sup>, J.A. Becker<sup>2</sup>, U. Agvaanluvsan<sup>2</sup>,  
M.B. Chadwick<sup>4</sup>, J.R. Cooper<sup>2</sup>, M. Devlin<sup>4</sup>, N. Fotiades<sup>4</sup>, P.E. Garrett<sup>2</sup>, R.O. Nelson<sup>4</sup>,  
C.Y. Wu<sup>2</sup>, W. Younes<sup>2</sup>

<sup>1</sup>North Carolina State University, Raleigh NC 27695, United States

<sup>2</sup>Lawrence Livermore National Laboratory, Livermore CA 94550, United States

<sup>3</sup>Triangle Universities Nuclear Laboratory, Durham NC 27708, United States

<sup>4</sup>Los Alamos National Laboratory, Los Alamos NM87545, United State

## Abstract

Cross-section measurements were made of prompt gamma-ray production as a function of incident neutron energy ( $E_n = 1$  to 35 MeV) on an enriched (95.6%)  $^{150}\text{Sm}$  sample. Energetic neutrons were delivered by the Los Alamos National Laboratory spallation neutron source located at the Los Alamos Neutron Science Center (LANSCE) facility. The prompt-reaction gamma rays were detected with the large-scale Compton-suppressed Germanium Array for Neutron Induced Excitations (GEANIE). Neutron energies were determined by the time-of-flight technique. The  $\gamma$ -ray excitation functions were converted to partial  $\gamma$ -ray cross sections taking into account the dead-time correction, target thickness, detector efficiency and neutron flux (monitored with an in-line fission chamber). Partial  $\gamma$ -ray cross sections were predicted using the Hauser-Feshbach statistical reaction code GNASH. Above  $E_n \sim 8$  MeV the pre-equilibrium reaction process dominates the inelastic reaction. The spin distribution transferred in pre-

\* LLNL L-414 P.O.Box 808

Livermore, CA 94551

Tel: 1-925-422-7753; Fax 1-925-422-5940

Email: [dashdorj1@llnl.gov](mailto:dashdorj1@llnl.gov) (Dugersuren Dashdorj)

equilibrium neutron-induced reactions was calculated using the quantum mechanical theory of Feshbach, Kerman, and Koonin (FKK). These pre-equilibrium spin distributions were incorporated into a new version of GNASH and the  $\gamma$ -ray production cross sections were calculated and compared with experimental data. The difference in the partial  $\gamma$ -ray cross sections using spin distributions with and without pre-equilibrium effects is discussed.

PACS: 21.10.-i, 24.60.Dr, 25.40.-h, 25.40.Fq, 27.40.+z

Keywords:  $\gamma$ -ray production cross section, pre-equilibrium reaction, GEANIE, Feshbach-Kerman-Koonin, Sm-150

## 1. Introduction

Analysis of  $\gamma$ -ray production cross section measurements at LANSCE performed with the GEANIE detector array [1] demonstrated that the spin distribution has a large impact on the  $\gamma$ -ray transition probability when a high-spin state is involved [2,3]. Since it was assumed that the spin distribution in the pre-equilibrium process has a rather limited impact on nuclear reaction cross sections, classical theories such as the exciton model [4, 5] are still widely used to analyze particle emission data at high incident energies. A realistic treatment of the spin distribution should improve the accuracy of calculations of  $\gamma$ -ray production cross sections with the statistical Hauser-Feshbach model including the pre-equilibrium reaction mechanism. There are several well-known statistical multistep direct (MSD) theories: Feshbach, Kerman, and Koonin [6] (FKK), Tamura, Udagawa, and Lenske [7] (TUL), and Nishioka, Weidenmüller, and Yoshida [8] (NWY). These theories employ different statistical assumptions for the multistep reactions. However, descriptions of the first step (one-step) are very similar in principle [9]. The statistical

assumptions employed in these various theories are still under debate, but differences between the theories occur mainly in reactions at high incident energies. At low energies ( $E < 20$  MeV), the one-step process and the multistep compound (MSC) process can be employed to analyze experimental data.

Neutron inelastic scattering populates excited states by (1) forming the compound nucleus and decaying by neutron emission, or (2) by the incoming neutron transferring energy to create a particle-hole pair, and thus initiating the pre-equilibrium process. These two processes produce rather different spin distributions. The momentum transfer via the pre-equilibrium process tends to be smaller than in the compound reaction. This difference in the spin population has a significant impact on the de-excitation by  $\gamma$ -ray cascading.

We present comparisons of  $\gamma$ -ray production cross sections for neutron-induced reactions on  $^{150}\text{Sm}$ . The spin-distribution in the pre-equilibrium process is calculated with the FKK model, and the calculated spin-distribution is combined with the GNASH Hauser-Feshbach statistical model calculations [10]. To examine the influence of the FKK calculation, we also consider the case with the spin-distribution in the pre-equilibrium process the same as for the compound process. In the past such an assumption has often been made for Hauser-Feshbach plus exciton model calculations.

## 2 Experimental methods and Data analysis

Cross-section measurements were made of prompt  $\gamma$ -ray production as a function of incident neutron energy ( $E_n = 1$  to 35 MeV) on an enriched (95.6%)  $^{150}\text{Sm}$  sample. Energetic neutrons were delivered by the Los Alamos National Laboratory spallation neutron source located at the LANSCE/WNR facility. A natural W target was bombarded by the 800-MeV pulsed-proton beam from the LANSCE linear accelerator. The proton beam consisted of micropulses 1.8  $\mu\text{s}$  or

1 3.6  $\mu\text{s}$  apart bunched into macropulses 625  $\mu\text{s}$  in length. As a result of the spallation reactions,  
 2 neutrons with energies from a few keV to nearly 800 MeV are produced. The prompt-reaction  
 3  $\gamma$  rays were detected with the GEANIE array. The GEANIE spectrometer [1] is located about 20  
 4 m from the neutron source on the  $60^\circ$  right flight path. GEANIE consists of 11 LEPS and 15  
 5 coaxial detectors. All of the LEPS detectors and 9 of the coaxial detectors were equipped with  
 6 BGO suppression shields. The LEPS detectors were used to measure  $\gamma$ -rays with energies less  
 7 than 1 MeV and coaxial detectors  $\gamma$ -rays with energies up to 3 MeV. The neutron flux is  
 8 monitored by in-beam  $^{235,238}\text{U}$  fission chambers, located 2 m upstream from the array.  
 9 The incident neutron energy was determined by the standard time-of flight (TOF) technique. The  
 10 data were collected with 1.8  $\mu\text{s}$  spacing between macropulses for about 10 days with a 7.5 gm,  
 11 2.54-cm diameter,  $^{150}\text{Sm}_2\text{O}_3$  target enriched to 95.6% in  $^{150}\text{Sm}$ . In addition, 3 days of data with  
 12 the same target were collected with 3.6  $\mu\text{s}$  spacing between micropulses. During data playback,  
 13 events were separated into in-beam and out-of-beam matrices, and 2D matrices for  $E_\gamma$  vs. TOF  
 14 were generated. The energy calibration was performed using the energies of known transitions in  
 15  $^{150}\text{Sm}$  and other isotopes in the in-beam data.

16 The excitation functions were obtained by applying 15-ns-wide TOF gates on the  $\gamma$ -ray events in  
 17 the interval  $E_n = 1$  to 35 MeV. Detector efficiencies were calculated using MCNP [11]. Separate  
 18 experimental runs were also performed with the same setup and with the same target sandwiched  
 19 between iron foils. The partial  $\gamma$ -ray cross section for the 847-keV transition from the  $2^+$  to the  
 20 ground state in  $^{56}\text{Fe}$  was extracted and compared to the evaluated cross section at  $E_n=14.5$  MeV  
 21 [12]. The partial cross section extracted for the  $2^+$  to  $0^+$  transition from data was consistent,  
 22 within errors, with previous work.

### 3 Theoretical calculations

The  $\gamma$ -ray production cross sections are calculated with the GNASH code [10]. GNASH calculates the pre-equilibrium process with the exciton model, which is based on a classical theory and does not calculate spin transfer. We employ the exciton model for the pre-equilibrium strength calculation, but then modify the spin-distribution as calculated with the FKK theory. The MSD calculation employed is similar to the modeling of Koning and Chadwick [13], and is reported elsewhere [14]. In the present analysis, the MSC component is assumed to have the same spin distribution as the compound process, because it has a weak dependence on the angular distribution, and the magnitude is usually smaller than MSD [15].

The one-step calculation of MSD gives a spin-dependent population of continuum states in  $^{150}\text{Sm}$ . Since the ground state spin of  $^{150}\text{Sm}$  is zero, the spin distribution in the continuum populated by the one-step process is the same as the J-dependence of the MSD angle-integrated cross sections. We also calculate the population by a pure compound reaction. The initial population of  $^{150}\text{Sm}$  (after neutron inelastic scattering, but before  $\gamma$ -ray cascading) is a sum of pre-equilibrium and compound contributions.

The calculated one-step FKK spin-distributions are expressed by a Gaussian form. An example is shown in Fig. 1, which is a calculated spin-distribution for the  $^{150}\text{Sm}$  inelastic scattering at neutron incident energy of 20 MeV and emitted neutron energy of 11 MeV. The solid histogram is the FKK result, and the dotted histogram is the spin-distribution of the compound reaction. The FKK spin distribution is peaked at lower J-values; a high-spin state is difficult to make with a simple lp-lh configuration in a single-particle model. We fitted the Gaussian form to the FKK results with various neutron incident / out-going energies to obtain spin-cutoff parameters as a function of excitation energy  $E_n$ .

The particle transmission coefficients were calculated using the global optical potentials of Koning and Delaroche [16] for neutrons and protons, and the  $\alpha$ -particle optical potential of Avrigeanu, Hodgson, and Avrigeanu [17] was adopted for the  $\alpha$  particles. The direct inelastic scattering cross sections were calculated using the DWBA method.

The level scheme of  $^{150}\text{Sm}$  and the  $\gamma$ -ray branching ratios were taken from the Table of Isotopes [18] and RIPL-2. We included the discrete levels of  $^{150}\text{Sm}$  up to 1.836 MeV ( $8^+$ ).

The spin-distribution in the initial population is given by

$$R(E_x, J) = f_p(E_x) R_{PE}(E_x, J) + (1 - f_p(E_x)) R_{CN}(E_x, J), \quad (1)$$

where  $R_{PE}$  and  $R_{CN}$  are the spin-distributions for the pre-equilibrium and compound processes,  $f_p(E_x)$  is the fraction of pre-equilibrium to the total neutron emission. Because we assumed that MSC has the same spin-distribution as CN,

$$R(E_x, J) = [f_p(E_x) - f_c(E_x)] R_{MSD}(E_x, J) + [1 - f_p(E_x) + f_c(E_x)] R_{CN}(E_x, J), \quad (2)$$

where  $f_p(E_x)$  is the fraction of MSC, and  $R_{MSD}$  is given by the Gaussian form of one-step FKK spin-distributions. The fraction of pre-equilibrium cross section  $f_p(E_x)$  is calculated with the exciton model.

Figure 2 shows the spin-distributions in the continuum of  $^{150}\text{Sm}$  that is excited by 20-MeV neutron inelastic scattering. In past nuclear model calculations, the spin-distribution in the pre-equilibrium process has been assumed to be the same as in the compound reaction. This is illustrated in the top panel of Fig 2. With the quantum mechanical theories of the pre-equilibrium process, the spin-distribution can be calculated on a more realistic basis. This is shown in the bottom panel. The excited nucleus has a spin-distribution that is peaked at lower J-values when the excitation energy of the residual state is not too high.

## 4 Results and Conclusions



The spin distribution of the pre-equilibrium process in  $^{150}\text{Sm} + n$  reactions was calculated using the quantum mechanical theory of FKK. The FKK spin distribution was incorporated into GNASH calculations and the  $\gamma$ -ray production cross sections were calculated and compared with experimental data. Comparisons of the partial  $\gamma$ -ray cross sections for the 334-keV ( $2^+$  to  $0^+$ ), 439-keV ( $4^+$  to  $2^+$ ), 505-keV ( $6^+$  to  $4^+$ ), and 558-keV ( $8^+$  to  $6^+$ ) ground state band transitions in  $^{150}\text{Sm}$  are shown in Fig. 3. The difference in the cross sections between including spin distributions with and without pre-equilibrium effects is significant. The probability of  $\gamma$ -ray transitions from a high spin state is strongly suppressed because of the pre-equilibrium spin distribution. The difference in the partial  $\gamma$ -ray cross sections using spin distributions with and without pre-equilibrium effects was significant, e.g., for the 558-keV transition between  $8^+$  and  $6^+$  states the calculated  $\gamma$ -ray production cross sections changed by 70% at  $E_n = 20$  MeV with the inclusion of the pre-equilibrium spin distribution.

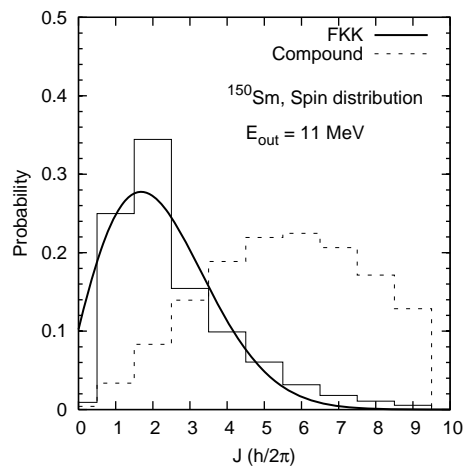
### Acknowledgments

This work was supported in part for NCSU/TUNL by the U.S. Department of Energy Grants No. DE-FG52-06NA26194 (NNSA Academic Alliance) and No. DE-FGO2-97-ER41042. This work was performed, in part under the auspices of the U.S. DoE by University California, Lawrence Livermore National Laboratory under contract Nos. W-7405-ENG-48. Work performed, in part, under the auspices of the U.S. DoE by Los Alamos National Security, LLC, Los Alamos National Laboratory under Contract No. DE-AC52-06NA25396.

### References

[1] J.A. Becker, R.O. Nelson, Nucl. Phys. News Int. **7**, p.11 (1997).

- 1    [2] T. Kawano, P. Talou, M.B. Chadwick, [to be published in Nucl. Instr. Methods A (2006)]
- 2    [3] D. Dashdorj, Ph.D thesis, North Carolina State University, (2005).
- 3    [4] J.J. Griffin, Phys. Rev. Lett. 17, 478 (1966).
- 4    [5] E. Gadioli, P.E. Hodgson “Pre-Equilibrium Nuclear Reactions,” Clarendon Press, Oxford
- 5    (1992).
- 6    [6] H. Feshbach, A. Kerman, S. Koonin, Ann. Phys. (N.Y.) 125, 429 (1980).
- 7    [7] T. Tamura, T. Udagawa, H. Lenske, Phys. Rev. C **26**, 379 (1982).
- 8    [8] H. Nishioka, H.A. Weidenmüller, S. Yoshida, Ann. Phys. (N.Y.) 183, 166 (1988).
- 9    [9] A.J. Koning, J.M. Akkermans, Ann. Phys. (N.Y.) 208, 216 (1991).
- 10   [10] P.G. Young, E.D. Arthur, M.B. Chadwick, LA-12343-MS, Los Alamos National Laboratory
- 11   (1992).
- 12   [11] D. P. McNabb, UCRL-TR-139906, Lawrence Livermore National Laboratory (1999).
- 13   [12] R. O. Nelson et al., *Proc. Int. Conf. Nuclear Data for Science and Technology*, Santa Fe,
- 14   USA, 26 Sep — 1 Oct, p.838 (2004).
- 15   [13] A.J. Koning, M.B. Chadwick, Phys. Rev. C **56**, 970 (1997).
- 16   [14] T. Kawano, T. Ohsawa, M. Baba, T. Nakagawa, Phys. Rev. C **63**, 034601 (2001).
- 17   [15] I. Kawano, Phys. Rev. C **59**, 865 (1999).
- 18   [16] A. Koning, J.-P. Delaroche, Nucl. Phys. **A713**, 231 (2003).
- 19   [17] V. Avrigeanu, P. Hodgson, M. Avrigeanu Phys. Rev. C **49**, 2136 (1994).
- 20   [18] R.B. Firestone, “Table of Isotopes,” Eighth Edition, John Wiley & Sons, Inc. (1998).

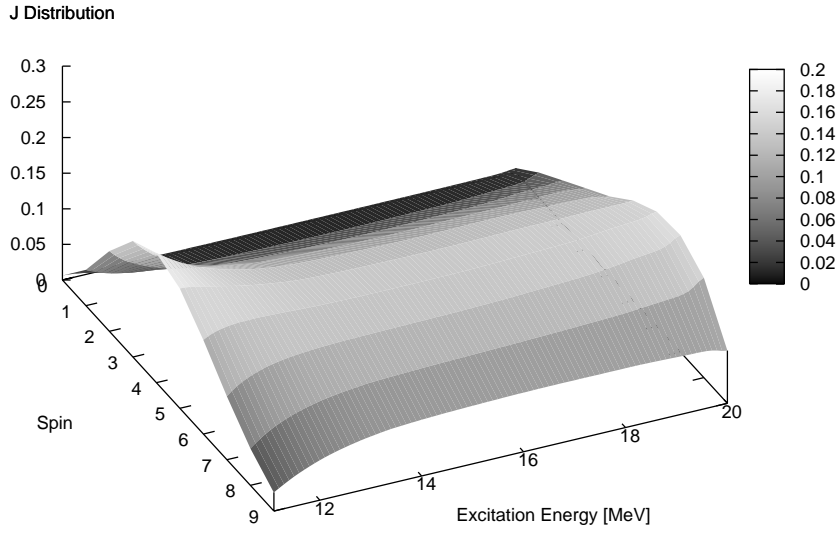


1

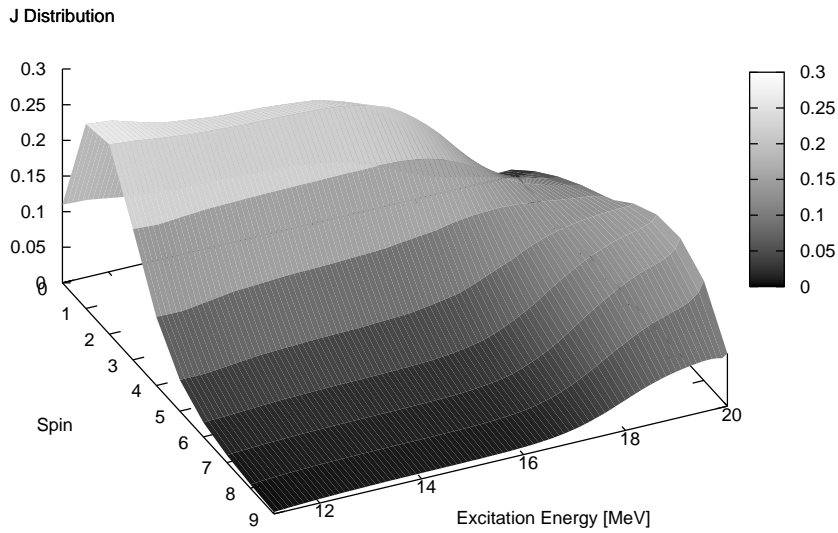
2 Figure 1: Comparison of the spin-distribution for the  $E_{\text{in}} = 20 \text{ MeV}$  and  $E_{\text{out}} = 11 \text{ MeV}$  process,

3 calculated with the FKK model (solid histogram), and the compound reaction (dotted histogram). The

4 smooth curve is a Gaussian fit to the FKK result.

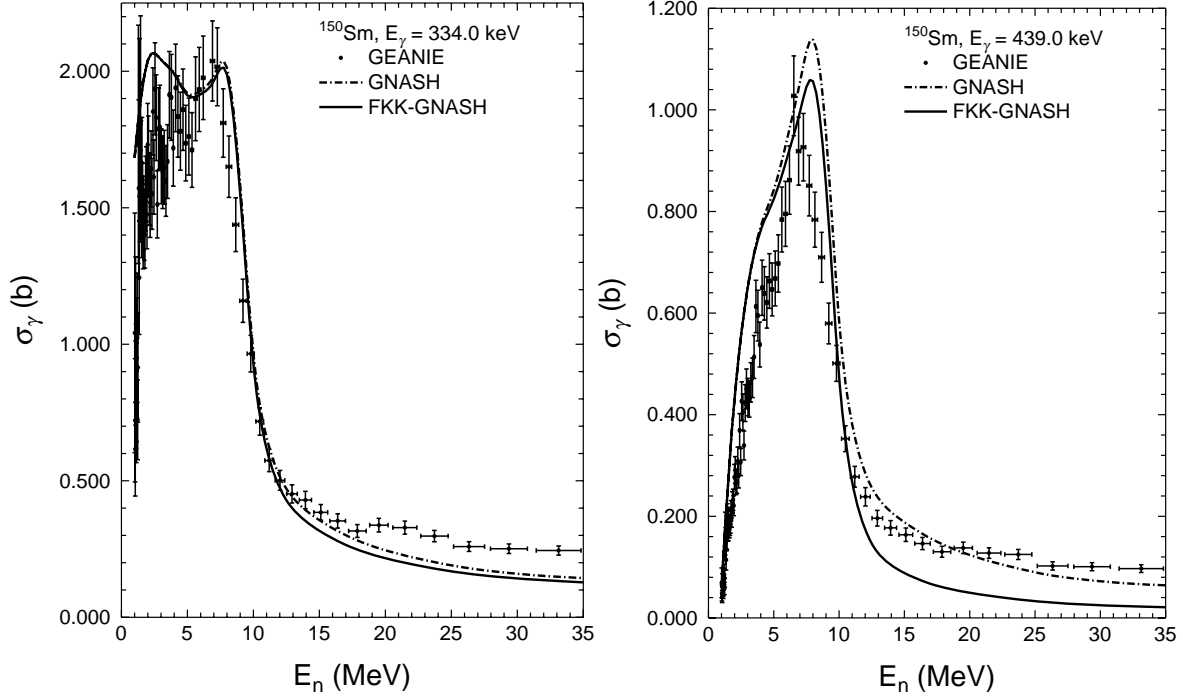


1

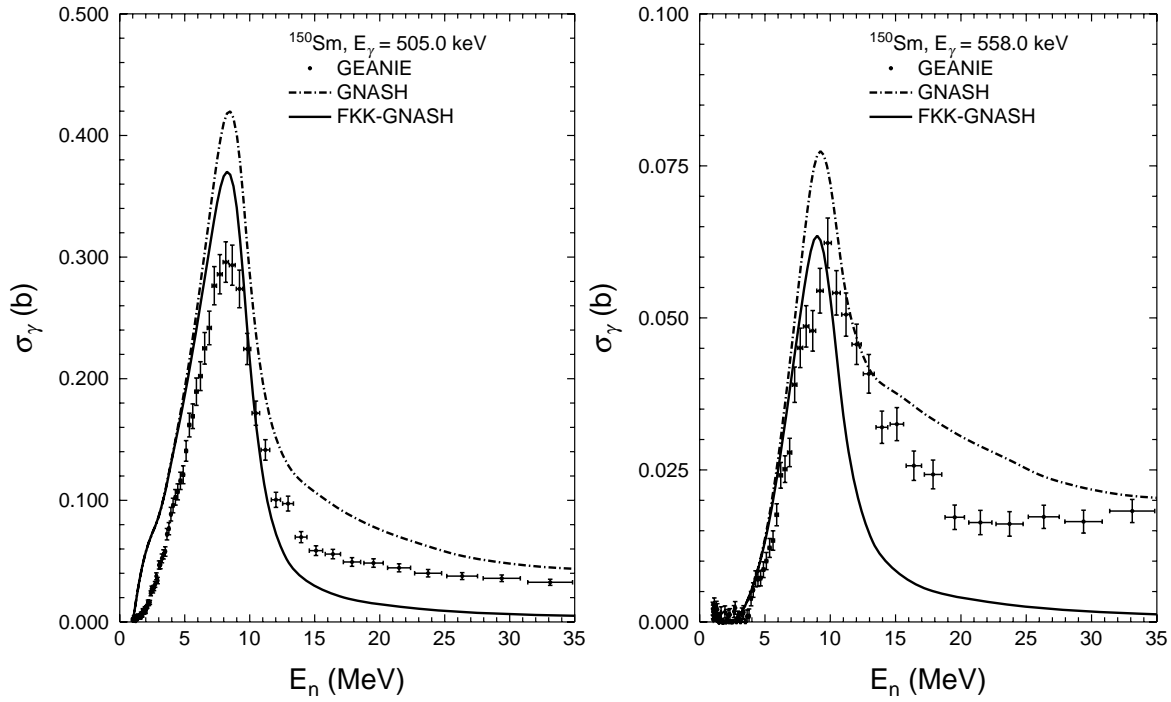


2

Figure 2: The spin distributions in excited  $^{150}\text{Sm}$  after neutron inelastic scattering, with different assumptions for the pre-equilibrium spin transfer. The neutron incident energy is 20 MeV. The upper panel shows the case when the pre-equilibrium spin distribution is assumed to be the same as the compound reaction. The bottom panel is the case when the FKK spin distribution is included in the GNASH calculations.



1



2

3 Figure 3: Comparison of the 334-, 439-, 505-, and 558-keV  $\gamma$ -ray production cross sections with  
 4 calculations. The solid line represents the FKK+GNASH calculation, and the dashed line

- 1 represents the case where the pre-equilibrium spin-distribution is assumed to be the same as for
- 2 the compound reaction.